Polish Journal of Chemical Technology, 18, 2, 97—103, 10.1515/pjct-2016-0035

Impact of membrane pore structure on protein detection sensitivity of affinity-based immunoassay

A.L. Ahmad[1*], N. Ideris[2], B.S. Ooi[1], S.C. Low[1], A. Ismail[3]

[1]*Universiti Sains Malaysia, School of Chemical Engineering, Engineering Campus, Seri Ampangan, 14300 Nibong Tebal, S.P.S, Penang, Malaysia*
[2]*Universiti Teknologi MARA, Faculty of Chemical Engineering, 40450 Shah Alam, Selangor, Malaysia*
[3]*Universiti Sains Malaysia, Institute for Research in Molecular Medicine, Health Campus, 16150 Kubang Kerian, Kelantan, Malaysia*
[*]*Corresponding author: e-mail: chlatif@usm.my*

Understanding a membrane's morphology is important for controlling its final performance during protein immobilization. Porous, symmetric membranes were prepared from a polyvinylidene fluoride/N-methyl-2-pyrrolidinone solution by phase inversion process, to obtain membrane with various microsized pores. The concentration and surface area of aprotein dotted on the membrane surface were measured by staining with Ponceau S dye. The dotted protein was further scanned and analysed to perform quantitative measurements for relative comparison. The intensity of the red protein spot and its surface area varied depending on the membrane pore size, demonstrating the dependence of protein immobilization on this factor. The membrane with the smallest pore size (M3) showed the highest protein spot intensity and surface area when examined at different protein concentrations. An increase in the applied protein volume showed a linearity proportional trend to the total surface area, and an uneven round dot shape was observed at a large applied volume of protein solution.

Keywords: morphology, PVDF membrane, protein immobilization.

INTRODUCTION

The advancement of modern medical technology plays a critical role in saving human lives through improved treatment and control of the spread of diseases. However, the annual rate of mortality is very high, especially in underdeveloped or developing countries, mainly because of the scarcity of medical resources such as highly trained specialists and advanced diagnostic equipment[1]. The available technologies are mostly limited to an urban setup and require a long waiting period for access. Hence, to address these issues, sensitive, affordable, and efficient diagnostic tool kits are desirable to assist untrained medical workers and offset the unavailability of non-portable high-end technology in rural areas. Usually, diagnostic tool kits are functionally based on the concept of immunoassays, such as those used in the initial screens for HIV[2, 3], tuberculosis[4], typhoid[5], and malaria. Another example would be the very commonly available pregnancy test strip[6].

Immunoassays are antibody-based detection systems for specific antigens, and their efficiency originates from the considerable specificity of an antibody for its particular antigen. The assays function by measuring the concentration of a substance in a complex biological liquid system, typically serum or urine. In a homogenous immunoassay, the antigen, antibody, and sample are mixed in the solution phase. In contrast, in a heterogeneous assay, one constituent is immobilized on a solid surface, while the other constituents are delivered via the solution phase[7, 8]. A heterogeneous assay is always an attractive choice for overcoming the limitations of very low concentrations of biological markers in body fluids.

One of the important elements in an immunoassay is the use of a membrane as a capturing matrix. Heterogeneous immunoassays require a sorbent surface for the attachment of a protein reagent. Usually, a microporous polymeric membrane is selected as a sorbent surface because of the high binding affinity and stability of the biomolecules toward the substrate as well as the low cost of mass production[9]. A number of polymeric materials have been used to improve final assay performance, and membrane function may be controlled by manipulating the material behaviour during the fabrication process. Among the different types of polymers used, polyvinylidene fluoride (PVDF) has great potential[10], because of the high level of nonspecific interactions between the membranes and proteins. It is a commercially available polymeric material with special features such as thermal stability, low surface energy, and good physical, chemical, and mechanical properties[11]. Many reports have described applications of PVDF membranes as capture reagents in various immunoassays, including the detection of mycotoxins, mouse IgG and proteins[10, 12, 13].

The membrane pore structure has been shown to be a crucial factor affecting the accuracy and sensitivity of the immunoassay. Different pore structures or morphologies have been used, because specialized membrane materials, surface properties, structures and membrane dimensions have been required for different reagents in various downstream processes. Membranes with lower pore sizes exhibit enhanced protein immobilization in the membrane reaction zone, producing a more sensitive assay[14]. However, in addition to pore size, other factors such as porosity, pore connectivity, and tortuosity produce significant effects, as it is expected that the protein solution will not only diffuse horizontally but also vertically because of the effects of gravity.

Accordingly, in this study, we examined the detection sensitivity of various membrane morphologies on the affinity-based immunoassay, in consideration of different protein concentration and dot volumes. These observations are essential to analyse the membrane–protein immobilization behaviour in regards to the protein solution characteristics, and the physical properties of the

membranes. The improved understanding of the PVDF membrane morphology and downstream processes acquired in this study can be used in the future development of immunoassays with enhanced performance.

METHODOLOGY

Material

Homopolymer PVDF 6010, with a density of 1.78 g/cm^3, was supplied by Solvay Solexis (Brussels, Belgium). *N*-Methyl-2-pyrrolidinone (NMP, 99.5%) was purchased from Sigma-Aldrich (St. Louis, MO, US). Deionized water and 2-propanol (99.8%, Merck, Germany) were used as non-solvents during the phase inversion process. The protein (Bovine Serum Albumin) and Ponceau S protein staining solution (0.1% w/v Ponceau S and 5.0% w/v acetic acid) were supplied by Sigma-Aldrich. Potassium phosphate monobasic and dibasic anhydrous (Merck) were diluted in deionized water to prepare a phosphate buffer solution with a concentration of 0.05 M and pH 7.0. All the reagents were used without further purification.

Membrane preparation

Symmetrical, microporous PVDF membranes were prepared via non solvent-induced phase inversion according to a previously published method, with polymer concentrations of 13.0, 16.0, and 19 wt% (designated M1, M2 and M3 respectively)[15]. The casting process was performed at room temperature using an automatic film applicator (Elcometer 4340 Motorised, Elcometer, UK) with an initial casting thickness of 500 μm and a casting speed of 30 mm/s.

Membrane characterization

The pore size distributions (PSDs) of the membranes were measured by capillary flow porometry (Porolux 1000, Benelux Scientific, Belgium). In this method, the pressure needed to blow an inert gas through a liquid-filled membrane is measured, based on the Young–Laplace equation[16], with a maximum flow rate of 200 mL/min (Equation 1). For the measurement, each membrane sample was cut into pieces 2 cm in diameter and immersed in a perfluorinated wetting liquid (Porefil 12) for approximately 3 min before analysis.

$$\Delta P = \frac{2\gamma \cos\theta}{r} x\ 100\% \quad (1)$$

Where ΔP is the differential gas pressure, γ is the surface tension of the wetting liquid (12 dynes/cm), θ is the wetting angle, and r is the pore radius.

The surfaces of the membranes were further analysed by field emission scanning electron microscopy (FE-SEM, Supra 35VP, Carl Zeiss, Germany), using 1000× magnification. All membrane samples were coated with a Au–Pd alloy to enhance electronic conductivity and then observed by SEM at an acceleration voltage of 10 kV, with an SE2 detector. The yield thickness of the membrane samples was confirmed with a micro thickness gauge (Mitutoyo 7301, Japan) with an accuracy of 0.001 mm. At least five areas per sample were measured to confirm the reproducibility of the yield thickness. Finally, porosity differences among the synthesized membranes were calculated according to Equation 2, with 2-butanol (≥99.0%, Merck) as the immersion liquid[17].

$$\varepsilon = \frac{(W_B - W_M)/\rho_B}{(W_B - W_M)/\rho_B + W_M/\rho_P} x\ 100\% \quad (2)$$

Where W_B is the weight of the wet membrane, W_M is the weight of the dry membrane, ϱ_B is the specific gravity of 2-butanol (0.81 g/cm^3), and ϱ_P is the specific gravity of PVDF (1.78 g/cm^3).

Protein immobilization

Effect of protein concentration at different membrane pore sizes

The PVDF membrane was first cut into a 1 × 5 cm rectangle, and the upper surface was marked. The sample membrane was then soaked in ethanol for 15 sec at room temperature and placed on pre-wetted filter paper. In this study, Bovine Serum Albumin (BSA) was selected as a reference protein. The selection was contributed by its stability, its low cost and its lack of effect in many biochemical reactions[18]. Different concentrations of protein(1 μL at 0.3–10.0 mg/mL) were applied to membranes with varying pore sizes and left to dry in air[12]. After drying, the membrane was immersed in a sufficient amount of Ponceau S solution for 5 min. The membrane was then rinsed with deionized water to wash off the undesired membrane background and again air-dried at room temperature[19]. Ponceau S was selected as the protein stain because it has relatively low non specific binding (low background) to the PVDF membrane and is also a quick stain to indicate the binding capacity. Image acquisition of the dot blot was performed through SilverFast Launcher (v3.1.1), using an EPSON Perfection V700 scanner with the following settings: 16 > 8 bit grayscale and3200 dpi resolution. For protein quantification, Quantity One® basic (Version 4.6.9, Bio-Rad Laboratories) was used to measure the colour intensity and the total surface area. Each value represented an average of three spots[20].

Effect of protein volume

Different volumes of protein solution (0.5–5.0 μL) at constant concentration (3.0 mg/mL) were spotted on the membrane surface (M2) and left to air dry. Then, the membrane was stained with Ponceau S, scanned, and analysed by the image acquisition software, as described in the previous section.

RESULTS AND DISCUSSION

Prior to analyse the protein detection sensitivity, the synthesized membranes were characterized with respect to morphology. Figure 1 shows the wet and dry curves obtained via capillary flow porometry. For every sample,the wet and dry curves eventually coincided at a given pressure, which indicated that the samples were fully analysed. Based on the Laplace-Young equation, the pressure applied is inversely proportional to the pore radius (Equation 1); thus, a smaller pore size would require higher pressure to purge the wetting liquid from inside the membrane's pores. Theoretically, an abrupt increase in thepercentage flow is determined by

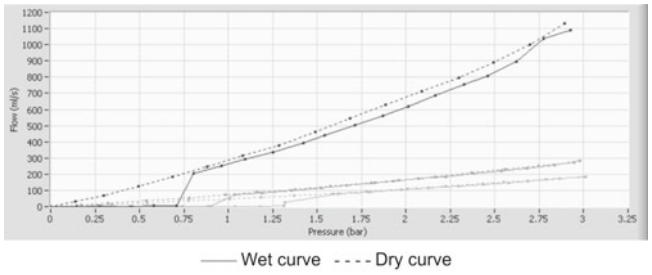

Figure 1. Wet and dry curves for membranes at different polymer concentration. M1 with 13 wt%, M2 with 16 wt% and M3 with 19 wt% of polymer concentration

an increase in the number of pores at a specific pore diameter. In other words, a sharp rise in the percentage flow indicates that the number of pores of a particular diameter is large. For the membrane with 13 wt% polymer concentration (M1), a sharp rise in the flow distribution was observed at a lower pressure, approximately 0.72 bar. As the polymer concentration increased to 16 and 19 wt%, the pressures required for the flow to jump were approximately 0.9 bar and 1.3 bar, respectively.

Figure 2 shows the percentage relative flowrates and the PSDs for all membrane samples. The percentage relative flowrates, presented in Figure 2(a), showed that all the samples reached 100% flow, indicating that the gas flow rates for wet and dry samples were equal at specific pressures. The steep slopes observed for all the samples corresponded to a narrow pore size distribution. As represented in Figure 2(b), the PSD of the 19 wt% polymer membrane was in the range ~0.21–0.26 μm. As the polymer concentration decreased, the PSDs increased to 0.28–0.38 μm and 0.35–0.48 μm for polymer concentrations of 16 and 13 wt%, respectively. Smaller PSDs (μm) showed a sharp peak and narrow base with a high percentage flow (%), indicating that most of the pore diameters were close to the mean. This also suggested that the membrane with smaller pores had better homogeneity throughout the sample layer. The membranes with larger pores exhibited broader PSDs, as can be observed from the wide base and low percent flow (%) of the 13 wt% polymer membrane sample.

The morphology analyses of the membranes were further supported by the FESEM micrographs, presented in Figure 3. The results were in accordance with the

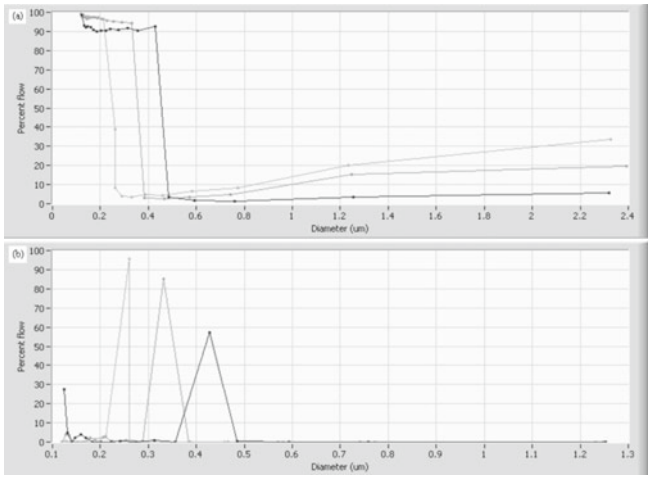

Figure 2. (a) Relative flow rate (%) and (b) Pore size distribution (%) for membranes of different polymer concentration. M1 with 13 wt%, M2 with 16 wt% and M3 with 19 wt% of polymer concentration

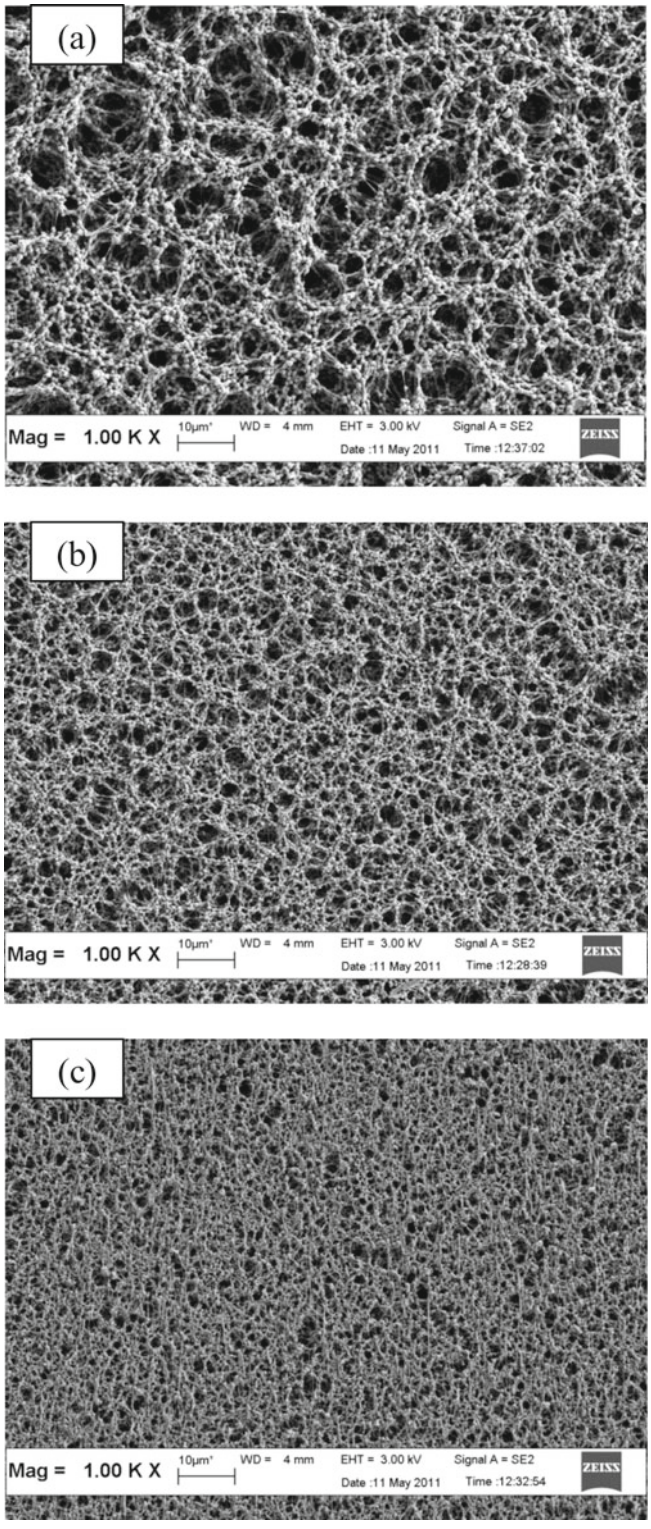

Figure 3. FESEM micrographs of membrane surface synthesized at different polymer concentration. (a) 13.0 wt% (b) 16.0 wt% and (c) 19.0 wt%

capillary flow porometry analysis: the PSD decreased as the polymer concentration increased. In general, the membrane morphology was composed of small, interconnected nodular structures. Fibril- and stick-like elements were observed to from bridged linkages between the nodules, which resulted in a tortuous maze of highly porous channels in the membrane structure. The mean pore sizes of the membranes are listed in Table 1, along with the porosity and yield thickness values. The relative porosities for all the membranes were calculated from Equation 2, and the yield thicknesses were measured using a micro thickness gauge.

Table 1. Mean pore size, porosity and yield thickness for membrane samples

Membrane Sample	Mean Pore Size [μm]	Porosity [%]	Yield Thickness [mm]
M1	0.4548	70.1002	0.0894
M2	0.3575	63.7580	0.0890
M3	0.2512	60.9757	0.1034

For protein immobilization analysis, Figure 4 represents the spot intensitiesof the membrane samples, M1 to M3, corresponding to PSDs of 0.4548 μm to 0.2515 μm. Each membrane was spotted witha volume of 1 μL with protein concentrations that ranged from 0.3 to 10.0 mg/mL. In general, all the membranes showed very low protein colour intensity at 0.3 mg/mL. The intensity became more significant as the protein concentration increased to 1.0 mg/mL, before reaching a nearly saturated intensity at approximately 0.35 when applied protein concentrations was more than 3.0 mg/mL. Less variation in absorbance readings is observed when the deposited protein concentration was more than 3.0 mg/ml for all membrane samples. This result was expected due to the saturation

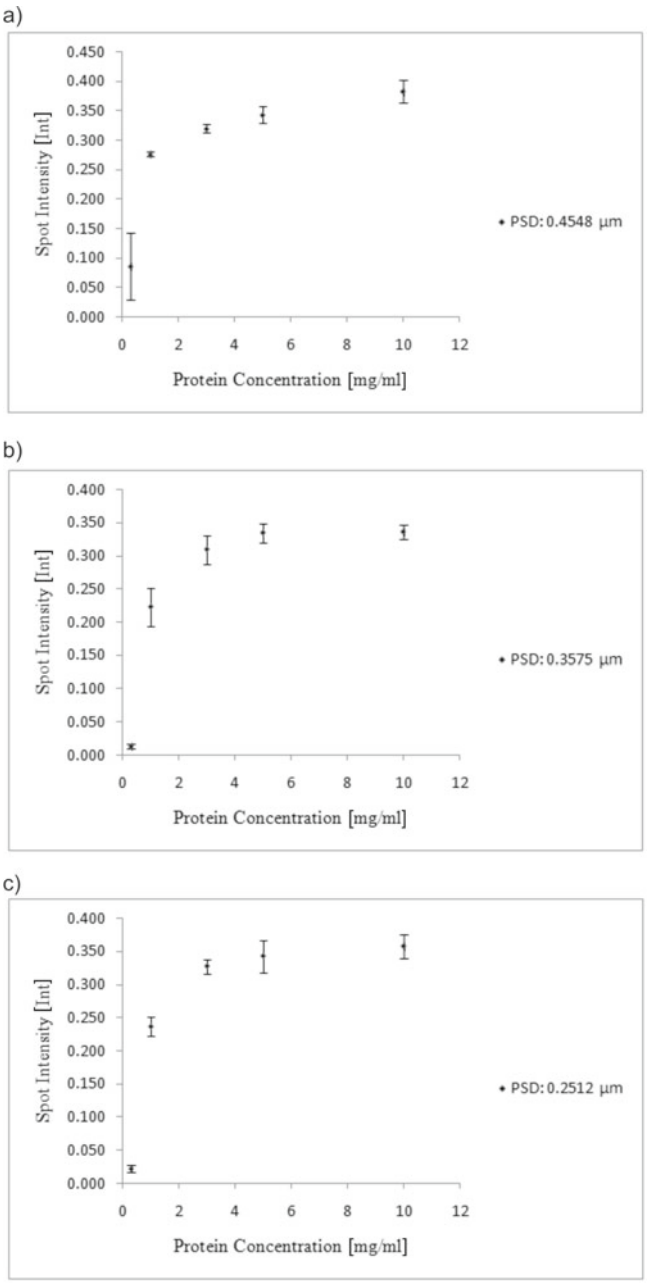

Figure 4. Spot intensity of the stained protein at different membrane pore size and protein concentration. (a) M1 (b) M2 (c) M3. (Volume 1 μL, pH 7)

of protein absorbing capacity on the membrane[21]. As long as the membrane reaches a saturated binding level, there will not be much different in the colour intensity regardless of the applied protein concentration.

At a close observation, 'coffee-ring' effect were observed when a lower protein concentrations (0.3 and 1.0 mg/mL) were immobilized. This is due to the uneven drying or evaporation of the dotted protein (Figure 5). As mentioned, after the membrane was dotted with the protein solution, it was left to air dry. As the drying process usually starts from the edge of the drop, the capillary flow of the protein solution carried the protein colloid particles outward from the centre of the spot. After evaporation was complete, the suspended protein particles were left highly concentrated along the original drop edge in a ring-like fashion, known as the coffee-ring effect[22]. However, this effect was only discernible at concentrations of 1.0 mg/mL and lower. It became less significant as the protein concentration increased. With concentrations of 3.0 mg/mL and higher, diffusion was the dominant transport mechanism in the system instead of capillary flow. According to Gorr et al[23] an increased in protein concentration will increase the crowding effect of particles through hydro-dynamic and direct interactions. Thus, the experimental diffusion coefficient values decreases as it inherently contain the effects of crowding or self-obstruction during the diffusion process. In a system with higher protein concentration (low protein diffusion coefficient), kinetic detention will be reached earlier as compared to lower concentration. Thus, a protein spot with higher concentration will undergo the gel transition earlier in the drying process and suppress the radial flow outward

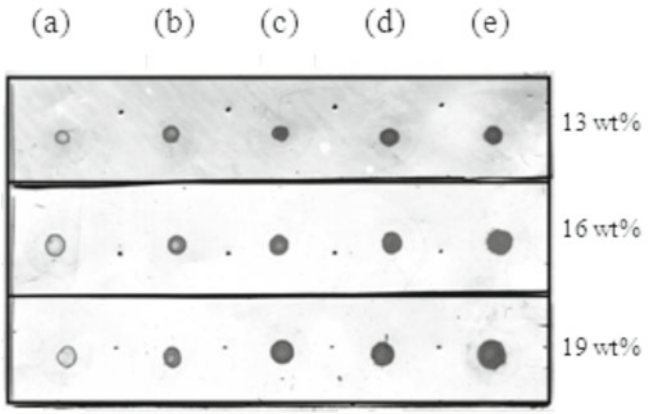

Figure 5. Stained protein spots (scanned at 16 > 8 bit grayscale and a resolution of 3200 dpi) on PVDF membrane at different pore size with varying protein concentration (a: 0.3 mg/ml b: 1.0 mg/ml c: 3.0 mg/ml d: 5.0 mg/ml e: 10.0 mg/ml)

In general, protein can bind onto the membrane surface by variety of mechanism, classified into hydrophobic interactions, electrostatic interactions, hydrogen bonding and van der Waals interactions[24]. However, among all the interactions, the most important driving forces for the

adsorption of protein are hydrophobic and electrostatic interactions[25, 26]. Hydrophobic interactions appear as the result of the dehydration of apolar (non polar) parts of the protein and the membrane while electrostatic interactions arise from coulombic attraction or repulsion between charged groups. The electrostatic effects are observed when the charges between the protein and the membrane surface are opposite, which, however, might be influenced by dilution or changing the pH. Electrostatic interactions are usually relevant on hydrophilic membrane or sorbent surface; and when repulsive, they may prevent the adsorption of protein at such hydrophilic surfaces[25].

However, on a hydrophobic surface such as PVDF membrane, the hydrophobic interaction dominates, allowing for high protein binding, even under electrostatically adverse conditions[27]. According to Liu et al[28], the strong hydrophobic interaction between the protein molecules on the hydrophobic PVDF membrane is that there are almost no hydrogen bonding interactions in the boundary layer between the PVDF membrane interface and water. The repulsion of water molecules away from hydrophobic PVDF membrane surface is spontaneous process and therefore protein molecules have a tendency to adsorb onto membrane surface and dominate the boundary layer.

For the same protein volume and concentration, the smallest pore size, M3, exhibiteda significant increase in the total surface area (mm^2), as compared to M1 and M2. As represented in Table 2, this observation became more noticeable as the protein concentration increased. As discussed earlier, M3 had a relatively narrow PSD, 0.21–0.26 μm, with an average PSD of 0.2512 μm. Thus, the immobilized protein was able to bind firmly and diffuse horizontally within the smaller pore matrix because there is more interconnecting polymer structures were formed within the membrane. Theoretically, a combination of smaller-pored membrane with high porosity would be desirable as a potential capture reagent, as it would be expected to offer a large surface area and good accessibility for protein adsorption[29]. Thus, it was found that M3 possessed a balanced combination of high porosity and small PSD to provide the largest interconnecting surface area for protein immobilization.

Meanwhile, M1, with a PSD of 0.4548 μm, exhibited consistently lower total surface area, along the increase of the protein concentration. This is mainly due to the inability of the protein to immobilize tightly on the membrane. Larger pores with a less interconnected polymer matrix (Fig. 3a) will reduce the affinity forces of the membrane-protein interaction and cause the protein to detach during the washing process. Additionally, a less interconnected matrix will cause the deposited protein solution to diffuse vertically because ofgravity. For these reasons, the resulting surface area would be reduced, instead of the broad and sharp protein spot observed for a membrane withsmaller pores.

Instead of protein concentration, the amount of immobilized protein on the membrane surface plays a key role in the development of an immunoassay, as the optimized volume of protein will maintain the sharpness and specificity of the immobilization. Previously, a constant volume of the protein solution was spotted onto the different membrane surfaces (M1, M2, and M3). Because all the membranes revealed the same trend of protein binding in terms of colour intensity, M2 was chosen as the substrate to examine the effects of different protein volumes. Figure 6 shows the effects of variable protein volumes applied at constant protein concentration to the membrane surface in terms of spot intensity and total surface area. At constant protein concentration, the amount of protein adsorbed remained the same regardless of the increasing protein solution volume spotted onto the membrane, as shown in Figure 6a. A slight increase in colour intensity could be observed when the protein volume increased. This insignificant increment of adsorption value could be due to the 'coffee ring' effect as described previously.

As expected, the increased volume of the protein solution contributed to the larger area of the immobilized protein (Fig. 6b). The resultant areas were linearly proportional to the volume of the protein solution, with an

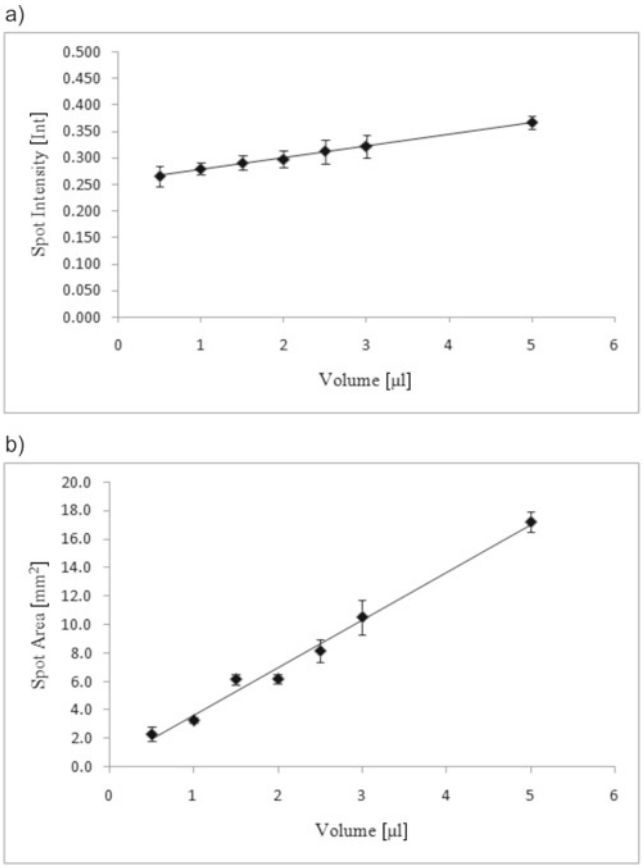

Figure 6. Spot intensity (a) and spot area (b) of the stained protein at different protein volume (Protein concentration 3.0 mg/ml, pH 7)

Table 2. Effect of membrane pore size on the spot area of the stained protein at different protein concentration

Membrane Sample / Protein Conc. [mg/ml]	Spot Area [mm^2]				
	0.3	1.0	3.0	5.0	10.0
M1 (0.4548 μm)	1.557 ±0.336	2.342 ±0.166	2.046 ±0.361	2.936 ±0.683	2.679 ±0.420
M2 (0.3575 μm)	2.620 ±0.169	2.584 ±0.089	2.997 ±0.207	3.217 ±0.275	4.265 ±0.253
M3 (0.2512 μm)	2.752 ±0.015	2.558 ±0.225	2.899 ±0.154	3.310 ±0.366	4.648 ±0.591

area of 17.191 mm^2 observed for a 5 μL protein volume. This was simply contributed by an increase in protein volume, which caused the solution to spread easily and made a bigger protein dot on the membrane. In this case, the protein solution spread to an extent defined by the partition coefficient between solid phase (membrane) and solute (protein solution). If higher volume is applied, the diffusion force in the solute will be greater and cause the solution to spread further. However, for that volume, the protein spot was uneven compared to lower protein volumes (Fig. 7). The uneven spreading of the protein was due to the interruption of protein flow in the polymer matrix. The excessive volume would result in poor contact for the membrane-protein interaction. Thus, the solution would diffuse to the available surface area and result inflow rate variations as the protein is immobilized on the membrane surface. Because the level of contact between the protein molecules and the membrane matrix is difficult to control, volume manipulation of the deposited protein is important to ensure an even dot on the membrane surface.

Figure 7. Stained protein spots (scanned at 16 > 8 bit grayscale and a resolution of 3200 dpi) on M2 at constant protein concentration (3.0 mg/ml) with varying protein volume (a: 0.5 μl b: 1.0 μl c: 1.5 μl d: 2.0 μl e: 2.5 μl f: 3.0 μl g: 5.0 μl)

CONCLUSIONS

In this study, we found that membrane morphology had a significant impact on protein capture when examined at different protein concentrations and volumes. The membrane with the smallest PSD, M3, exhibited the highest protein spot intensity and total surface area, as compared to membranes with bigger PSDs. Thus, M3 possessed a balanced combination of high porosity and small PSD, which offered the highest interconnecting surface area for protein immobilization. The coffee-ring effect was observed at concentrations of 1.0 mg/mL and lower for all membranes, because of the uneven drying or evaporation of the dotted protein. This effect left highly concentrated protein colloids along the original drop edge in a ring-like configuration. Increases in the applied protein volumes showed a linearly proportional trend to the total surface area. However, an excessive volume of protein solution (e.g., 5 μL) resulted in the formation of an unevenly round dot. Overall, the relationships between membrane morphology and protein immobilization behaviour were determined to understand fundamental membrane properties as decisive factors in the protein immobilization mechanism for immunoassays.

ACKNOWLEDGEMENTS

The authors acknowledge Universiti Sains Malaysia, USM (Vice-Chancellor Award 2010, USM-PGRS Grant (8034059), USM Membrane Cluster (8610012) and ERGS Grant (6730004) for financial support.

LITERATURE CITED

1. Wasunna, A.A. (2007). *Health Demands in Developing Country*. Pennsylvania, USA: Elsevier B.V.

2. Yuan, Z., Chen, W., Zhang, J., Zhang, J., Xiang, T., Hu, J., Wu, Z., Du, X., Huang, A. & Zheng, J. (2012). Development of an immunoassay for differentiating human immunodeficiency virus infections--from vaccine-induced immune response in Tiantan vaccine trials in China. Clin Biochem. 45(15), 1219–1224. DOI: 10.1016/j.clinbiochem.2012.05.013.

3. Ivo dos Santos, J., Galvao-Castro, B., Mello, D.C., Pereira, H.G. & Pereira, M.S. (1987). Dot enzyme immunoassay. A simple, cheap and stable test for antibody to human immunodeficiency virus (HIV). J. Immunol. Methods 99(2), 191–194. DOI: 10.1016/0022-1759(87)90126-8.

4. Attallah, A.M., Osman, S., Saad, A., Omran, M., Ismail, H., Ibrahim, G. & Abo-Naglla, A. (2005). Application of a circulating antigen detection immunoassay for laboratory diagnosis of extra-pulmonary and pulmonary tuberculosis. Clin Chim Acta 356(1–2), 58–66. DOI: 10.1016/j.cccn.2004.11.036.

5. Olsen, S.J., Pruckler, J., Bibb, W., Thanh, N.T.M., Trinh, T.M., Minh, N.T., Sivapalasingam, S., Gupta, A., Phuong, P.T., Chinh, N.T., Chau, N.V., Cam, P.D. & D.Mintz, E. (2004). Evaluation of rapid diagnostic tests for typhoid fever**.** J Clin. Microbiol. 42(5), 1885–1889. DOI: 10.1128/JCM.42.5.1885-1889.2004.

6. Albertini, A., Ghielmi, S. & Belloli, S. (1982). Structure, immunochemical properties and immunoassay of human chorionic gonadotropin. Ric. Clin. Laborat. 12(1), 289–298. DOI: 10.1007/BF02909335.

7. Debnath, M., Prasad, G.B.K.S. & Bisen, P.S. (2010). *Immunoassay*. Berlin, Germany: Springer Science+Business Media.

8. O'Sullivan, M.J. (2005). *Immunoassays*. Berlin, Germany: Springer Science+Business Media.

9. Ciardelli, G., Silvestri, D., Barbani, N., Ionita, M., Redaelli, A. & Giusti, P. (2006). Bioartificial polymer membranes as innovative systems for biomedical or biotechnological uses. Desalination 200(1–3), 493–495. DOI: 10.1016/j.desal.2006.03.408.

10. Aizawa, K. & Gantt, E. (1998). Rapid method for assay of quantitative binding of soluble proteins and photosynthetic membrane proteins on poly(vinylidene difluoride) membranes Anal. Chim. Acta 365(1–3), 109–113. DOI: 10.1016/S0003-2670(97)00670-3.

11. Ebnesajjad, S. (2000). *Fluoroplastics. Volume 1: Non-Melt Processible Fluoroplastics The Definitive User's Guide and Databook*. New York, USA: Plastics Design Library.

12. He, Q.H., Xu,Y., Wang, D., Kang, M., Huang, Z.B. & Li, Y.P. (2012). Simultaneous multiresidue determination of mycotoxins in cereal samples by polyvinylidene fluoride membrane based dot immunoassay. Food Chem. 134(1), 507–512. DOI: 10.1016/j.foodchem.2012.02.109.

13. Sulimenko, T. & Dráber, P. (2004). A fast and simple dot-immunobinding assay for quantification of mouse immunoglobulins in hybridoma culture supernatants. J. Immunol. Methods 289(1–2), 89–95. DOI: 10.1016/j.jim.2004.03.010.

14. Low, S.C., Ahmad, A.L., Ideris, N. & Ng, Q.H. (2011). Interaction of isothermal phase inversion and membrane formulation for pathogens detection in water. Biores. Technol 113, 219–224. DOI: 10.1016/j.biortech.2011.11.048.

15. Ahmad, A.L., Ideris, N., Ooi, B.S., Low, S.C. & Ismail, A. (2012). Synthesis of polyvinylidene fluoride (PVDF) membranes for protein binding: Effect of casting thickness. J. Appl. Polym. Sci. 128(5), 3438–3445. DOI: 10.1002/app.38522.

16. Kaur, S., Ma, Z., Gopal, R., Singh, G., Ramakrishna, S. & Matsuura, T. (2007). Plasma-induced graft copolymerization of Poly(methacrylic acid) on electrospun Poly(vinylidene fluoride) nanofiber membrane. Langmuir 23(26), 13085–13092. DOI: 10.1021/la701329r.

17. Nguyen, Q.T., Alaoui, O.T., Yang, H. & Mbareck, C. (2010). Dry-cast process for synthetic microporous membranes:

Physico-chemical analyses through morphological studies. J. Mem. Sci. 358(1–2), 13–25. DOI: 10.1016/j.memsci.2010.04.022.

18. El-Sharif, H.F., Stevenson, D., Warriner, K. & Reddy, S.M. (2014) *Hydrogel-based molecularly imprinted polymers for biological detection*. Berlin, Germany: Springer-Verlag.

19. Morçöl, T. & Subramanian, A. (1999). A red-dot-blot protein assay technique in the low nanogram range. Anal. Biochem. 270(1), 75–82. DOI: 10.1006/abio.1999.4057.

20. Ming, Li, D.L.P., Yvonne Cosgrove-Sweeney, Deena Ratner, Lisa C. Rohan, Alexander M. Cole, Patrick M. Tarwater, Phalguni Gupta and Bharat Ramratnam (2011). Incorporation of the HIV-1 microbicide cyanovirin-N in a food product. J. Acquir. Immune. Defic. Syndr. 58(4), 379. DOI: 10.1097/QAI.0b013e31823643fe.

21. Bannur, S.V., Kulgod, S.V., Metkar, S.S., Mahajan, S.K. & Sainis, J.K. (1999). Protein determination by Ponceau S using digital color image analysis of protein spots on nitrocellulose membranes. Anal. Biochem. 267(2), 382–389. DOI: http://dx.doi.org/10.1006/abio.1998.3020.

22. Yunker, P.J., Still, T., Lohr, M.A. & Yodh, A.G. (2011). Suppression of the coffee-ring effect by shape-dependent capillary interactions. Nature 476(7360), 308–311. DOI: 10.1038/nature10344.

23. Gorr, H.M., Zueger, J.M. & Barnard, J.A. (2012). Characteristic size for onset of coffee-ring effect in evaporating lysozyme-water solution droplets. J. Phys. Chem. B 116(40), 12213–12220. DOI: 10.1021/jp307933a.

24. Norde, W. (1999). *Proteins at Solid Surfaces*. New York, USA: Marcel Dekker Inc.

25. Giacomelli, C.E. (2006). *Adsorption of immunoglobulins at solid-liquid interfaces*. Boca Raton, Fla: Taylor & Francis.

26. Nakanishi, K., Sakiyama, T. & Imamura, K. (2001). On the adsorption of proteins on solid surfaces, a common but very complicated phenomenon. J. Biosci. Bioeng. 91(3), 233–244. DOI: 10.1016/S1389-1723(01)80127-4.

27. Norde, W. (1998). *Driving forces for protein adsorption at solid surfaces*. New York, USA: Marcel Dekker Inc.

28. Liu, F., Awanis Hashim, N., Liu, Y., Moghareh Abed, M.R. & Li, K. (2011). Progress in production and modification of PVDF membranes. J. Mem. Sci. 375(1–2), 1–27. DOI: 10.1016/j.memsci.2011.03.014.

29. Baker, R.W. (2003). *Membrane technology*. New Jersey, USA: A John Wiley & Sons Publication.